



ELSEVIER

Dynamics of Atmospheres and Oceans
36 (2002) 83–102

dynamics
of atmospheres
and oceans

www.elsevier.com/locate/dynatmoce

Cross-frontal transport along the Keweenaw coast in Lake Superior: a Lagrangian model study

Changsheng Chen^{a,*}, Jianrong Zhu^b, KiRyong Kang^c,
Hedong Liu^a, Elise Ralph^d, Sarah A. Green^e, Judith Wells Budd^f

^a School for Marine Science and Technology, University of Massachusetts-Dartmouth, 706 South Rodney French Boulevard, New Bedford, MA 02744-1221, USA

^b State Key Laboratory for Estuarine and Coastal Research, East China Normal University, Shanghai, China

^c Department of Marine Sciences, The University of Georgia, Athens, GA 30602, USA

^d Large Lake Observatory, University of Minnesota, Duluth, MN 55812-2496, USA

^e Department of Chemistry, Michigan Technological University, Houghton, MI 49931, USA

^f Department of Geological Engineering and Sciences, Michigan Technological University, Houghton, MI 49931, USA

Received 13 September 2000; received in revised form 28 January 2002; accepted 4 March 2002

Abstract

Offshore transport across the thermal front along the Keweenaw coast in Lake Superior was examined by tracking the trajectories of water particles in the model-simulated three-dimensional (3D) flow field of July 1973. Particles were released at different depths and horizontal locations within the Keweenaw Current during various wind events and were tracked until the end of the month. The trajectories of water particles showed a remarkable offshore cross-frontal water transport at the topographic-splitting point on the eastern side of the Keweenaw Waterway and near Eagle Harbor. This transport was driven dominantly by wind-induced Ekman flow near the surface but was controlled by local bottom topography in the deep region. A northeastward wind prevailed over the lake during July 1973. This wind tended to produce onshore water transports near the surface and hence caused downwelling against the coast. An offshore current was expected in the deep region based on the conservation of water mass. The vortex shedding off coastal bathymetry abutments plus baroclinic instability of the thermal front also led to offshore meandering of the temperature field in the deep region over local varying bottom topography. This meandering tended to produce a cyclonic vorticity and drove particles offshore across the thermal front along the northern coast of the Keweenaw Peninsula.

© 2002 Elsevier Science B.V. All rights reserved.

Keywords: Cross-frontal transport; Lagrangian model; Wind-induced Ekman flow

* Corresponding author.

E-mail address: c1chen@umassd.edu (C. Chen).

1. Introduction

The thermal front is one of the most important coastal physical structures in Lake Superior (Fig. 1a). This front usually establishes along the coast in late spring and intensifies in summer through fall as a result of the seasonal variation of surface solar heating and wind mixing over variable bottom slope (Smith and Ragotzkie, 1970; Bennett, 1978; Chen et al., 2001). Unlike low-salinity, tidal mixing, and shelfbreak fronts observed over the continental shelf, this front is located at a sharp slope close to the coast, with a cross-shore

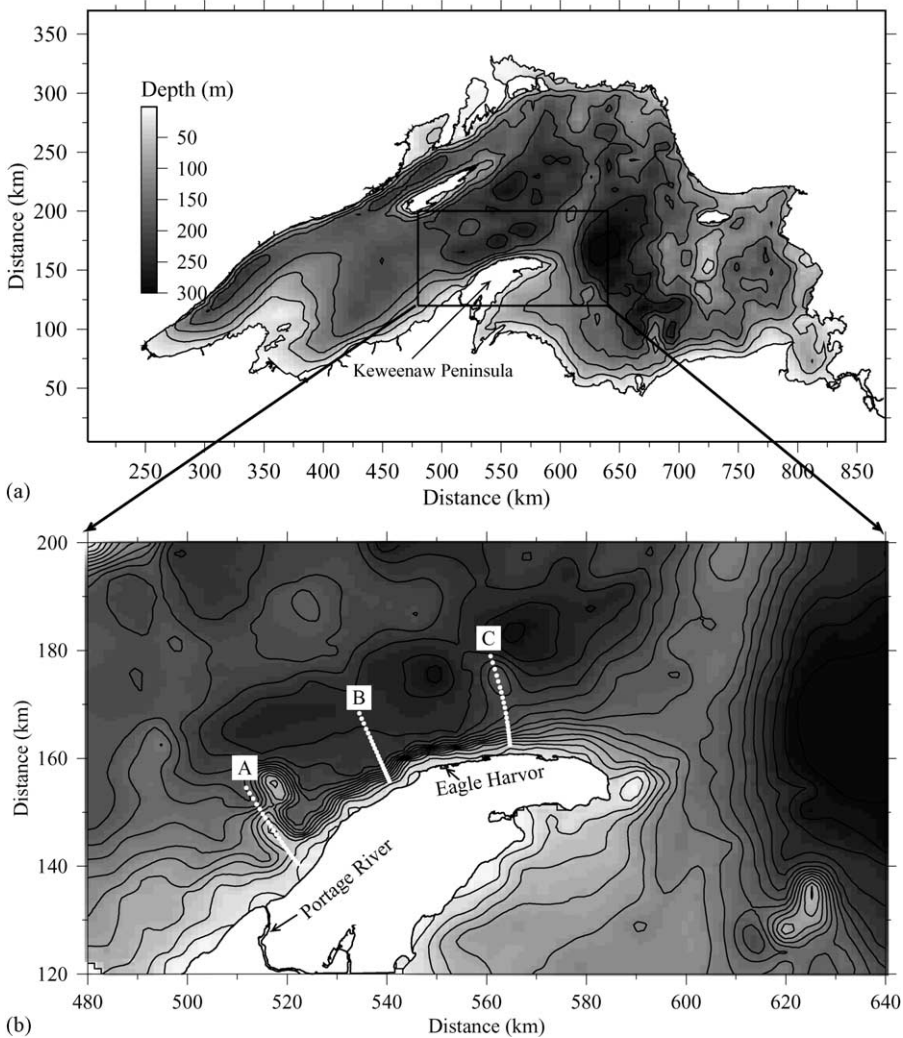


Fig. 1. Bottom topography (in meters) of Lake Superior (a), and the enlarged portion around the Keweenaw Peninsula (b). White solid lines are the locations of transects A, B, and C.

scale of less than 10 km (Niebauer et al., 1977; Chen et al., 2001; Zhu et al., 2001). The occurrence and evolution of this front has a direct impact on the coastal current jet along the Keweenaw Peninsula in Lake Superior (called the Keweenaw Current). This current jet weakens remarkably or intensifies significantly as the thermal front is advected offshore or onshore during periods of upwelling-favorable or downwelling-favorable wind. The maximum current speed can exceed 60 cm/s during a northeastward wind event in summer.

A comprehensive view of the thermal front and Keweenaw Current was given by Niebauer et al. (1977), and the physical processes that control the formation, evolution, and perturbation of this coastal front were examined recently by Chen et al. (2001) and Zhu et al. (2001). By using a three-dimensional (3D) prognostic numerical model, Chen et al. (2001) found that the thermal front along the coast of Lake Superior is baroclinically unstable, especially during wind relaxation. A significant energy transfer from the mean to perturbation flow causes an exponential growth of eddy kinetic energy, which leads to the formation of meso-scale eddies near the northeastern coast of the Keweenaw Peninsula. As a continuous work of Chen et al. (2001), Zhu et al. (2001) used the observed wind forcing plus monthly averaged heat flux to simulate successfully the 3D distribution of the Keweenaw Current recorded in July of 1973. They also found that surface solar heating plays a critical role in maintaining the thermal front and current jet along the Keweenaw coast during the summer. Because of a short distance to the coast, the front could be diffused offshore rapidly provided that no surface heat energy input exists.

Physical processes that cause cross-frontal water exchanges along the Keweenaw coast have not been well examined. Generally speaking, a thermal front along the coast acts like a dynamic barrier to momentum and offshore water transport. Water tends to move along the front and in the cross-shore direction the current is characterized by a double cell circulation, converging towards the front near the surface, sinking within the frontal zone, and diverging in the deep region, such that no cross-frontal water movement could occur (Chen et al., 2001). When either extra wind forcing or current shears exist, however, this barrier might be broken due to (1) temporal variation of surface winds (Oey, 1986; Chao, 1987; Blanton et al., 1989; Chen et al., 1999), and (2) baroclinic instability (Qiu and Imasato, 1988; Chen et al., 2001). Offshore cross-frontal water transport, therefore, could occur as episodic events along the coast.

In Lake Superior, the thermal front generally forms over a sharp slope near the northern coast of the Keweenaw Peninsula. The local isobaths are mainly parallel to the coastline, except east of the Keweenaw Waterway mouth (Portage River) and near Eagle Harbor where they extend offshore to form a subsurface sill in the cross-shore direction (Fig. 1b). Driven by wind perturbation or baroclinic instability, a large offshore meander of the thermal front may occur over these shallow abutments, thus leading to significant cross-frontal offshore water transport. Dynamics and kinematics of the cross-frontal water transport over variable bottom topography in Lake Superior, however, have not been explored prior to this current study.

In this paper, we examine the physical processes that control the cross-frontal offshore water transport along the Keweenaw Peninsula in Lake Superior. Three questions are addressed in this study: at first, where is the most active region for the cross-frontal offshore water removal? Second, what physical conditions cause offshore water transport to occur? Third, what is the role of variable bottom topography in cross-frontal water exchanges? To

answer these questions, a series of numerical experiments were conducted by tracking the trajectories of water particles under the flow field simulated by [Zhu et al. \(2001\)](#). Several process studies also were carried out to explore the kinematics associated with the thermal front over variable bottom topography.

2. The numerical model and experiment design

The numerical model used in this study is a 3D, non-orthogonal coordinate transformation, coastal ocean circulation model developed by [Chen et al. \(2001\)](#). This model is a modified version of the [Blumberg and Mellor \(1987\)](#) 3D primitive equation model with new non-orthogonal coordinates. The model incorporated a free surface for wave simulation and the [Mellor and Yamada \(1982\)](#) level 2.5 turbulent-closure sub-model for vertical mixing. The mathematical equations and numerical computational codes of the model were presented in detail by [Chen et al. \(2001\)](#) and a brief description of the model configuration is given here.

The model domain covered the entire volume of Lake Superior ([Fig. 2](#)), with higher resolution near the Keweenaw coast. The model grids were almost orthogonal in the interior of the lake except along the Keweenaw coast where non-orthogonal quadrilaterals were used to fit the shape of the coastline. The horizontal resolution was about 250–600 m in the cross-shore direction and about 4–6 km in the along-shore direction along the Keweenaw Peninsula. A σ -coordinate transformation (31 levels) was used in the vertical, which corresponds to a vertical resolution of about 1 m near the coast and 8.3 m at the 250-m isobath offshore. The time step of the numerical integration was 360 s.

The initial distribution of temperature was specified using observed temperature data taken regionally over the lake in late June ([Fig. 3](#)). Surface temperature was about 14 °C at the coast and decreased to 4 °C over a cross-shore distance of 5 km. The large horizontal and vertical temperature gradients only existed in the upper 60 m. The model was first spun up with the initial temperature field for 1 day, and then wind (increasing linearly from zero magnitude) was added on the second day to adjust the model-predicted current to the observed current on 1 July 1973. Driven by realistic surface wind stress ([Fig. 4](#)) and surface heat flux, the 3D fields of temperature and currents were simulated over a 1-month period starting at the end of the second model day. The model results for the simulation were described in detail in [Zhu et al. \(2001\)](#).

Particle trajectories were traced by solving the x , y , and z velocity equations:

$$\frac{dx}{dt} = u, \quad \frac{dy}{dt} = v, \quad \frac{d\sigma}{dt} = \frac{\varpi}{H + \zeta}, \quad (1)$$

where u , v , and ϖ are the x , y , and σ components of water velocity, respectively. The relation between ϖ and w is defined as

$$\varpi = w - (2 + \sigma) \frac{d\zeta}{dt} - \sigma \frac{dH}{dt}, \quad (2)$$

where w is the vertical velocity in the z -coordinate direction. The kinematic equations for u , v , and ϖ were calculated by means of a fourth-order Runge–Kutta scheme with a truncation

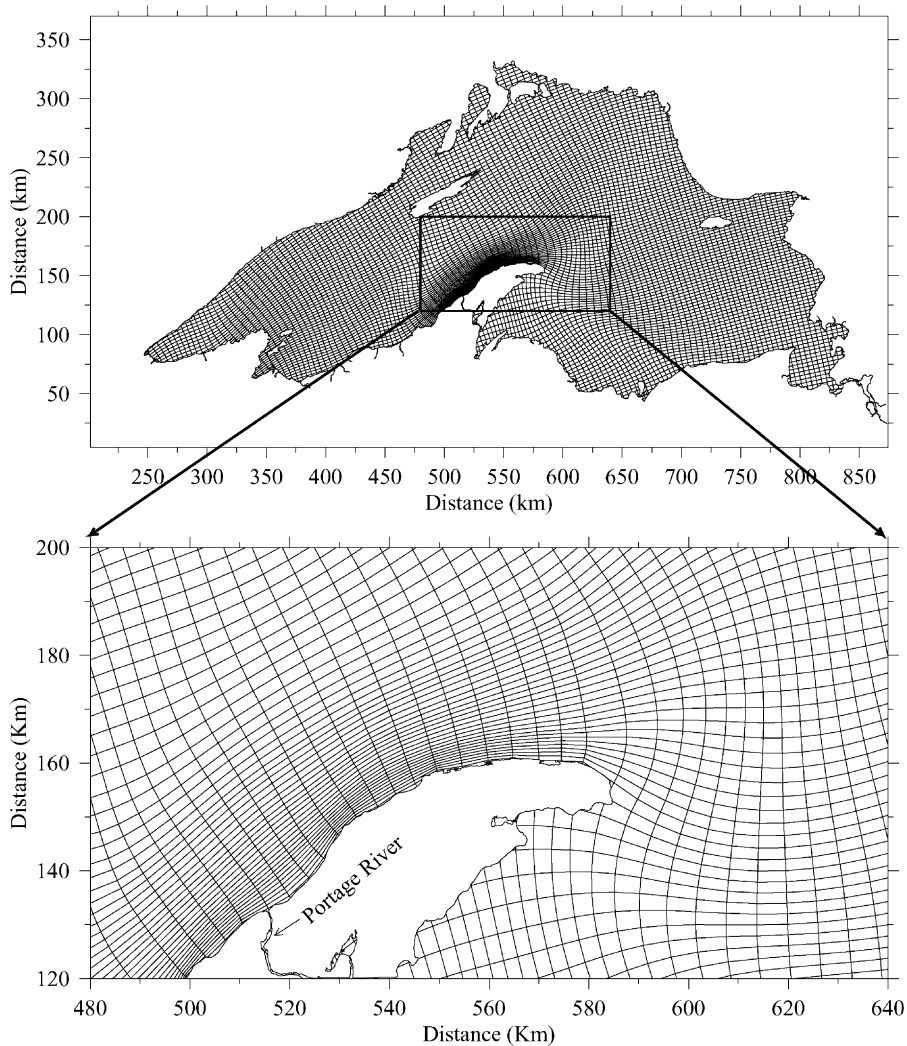


Fig. 2. Numerical grids of the Lake Superior model. The grids were almost orthogonal inside the lake except along the Keweenaw coast where non-orthogonal quadrilaterals were used to fit the shape of the coastline. The horizontal resolution is about 250–600 m in the cross-shore direction and about 4–6 km in the along-shore direction along the Keweenaw Peninsula.

error of order $(\Delta t)^5$. Particle velocities used in this calculation were obtained using a bilinear interpolation from eight nearest grid points. At each time step, each particle was checked to see if it was located inside the numerical domain. If a particle hit the bottom, it was kept there and no further tracking was carried out. We tracked particles in the model space (x, y, σ) and then converted their trajectories back to the physical space (x, y, z) . This method avoids the interpolation errors due to repeated transformations from σ - to z -coordinate systems.

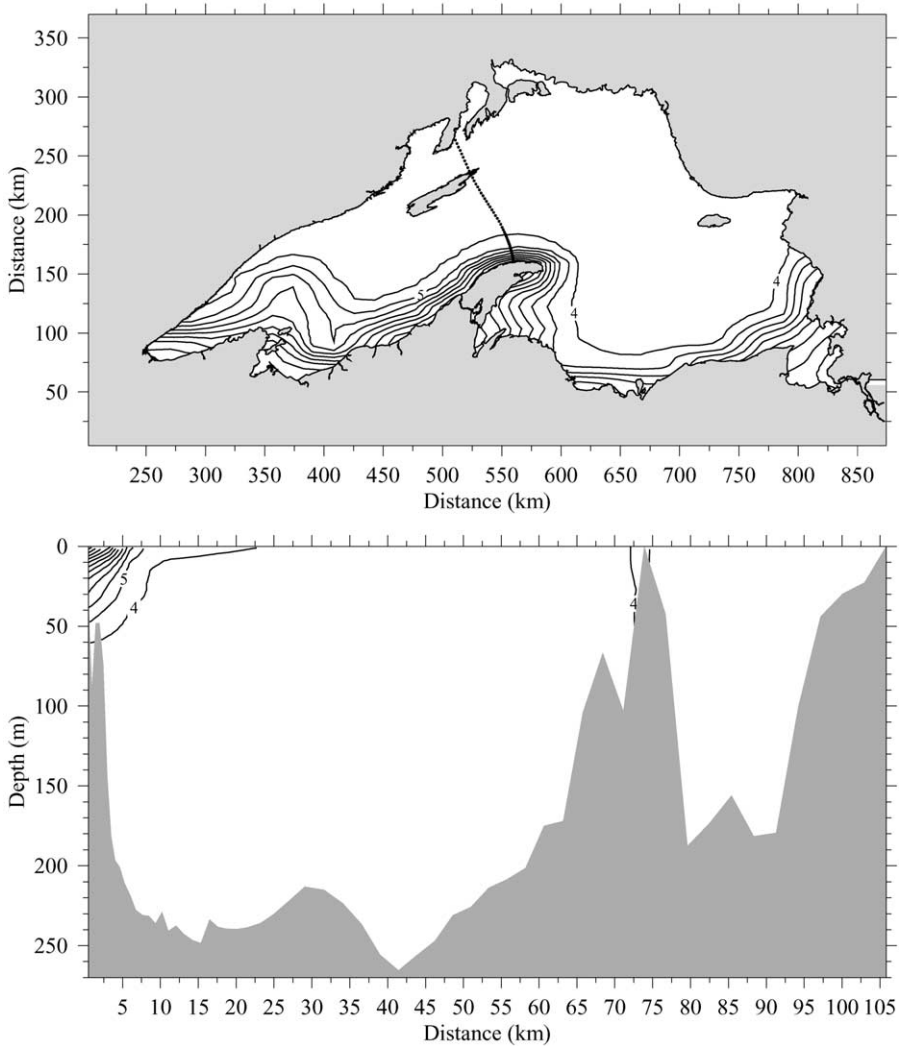


Fig. 3. Distributions of initial temperature at the surface (a), and on the cross-lake section (b). Dashed line in the upper panel indicates the location of the section used in the lower panel. The contour interval for temperature is 1°C .

3. The characteristics of particles' trajectories

The characteristics of the water movement along the Keweenaw coast were examined by tracking water particles under the 3D flow field of July 1973. Particles were released every 10 m in the vertical on cross-shore transects A, B, and C on the 2 July. The total number of particles released on transect A was 114. These particles tended to move eastward along the

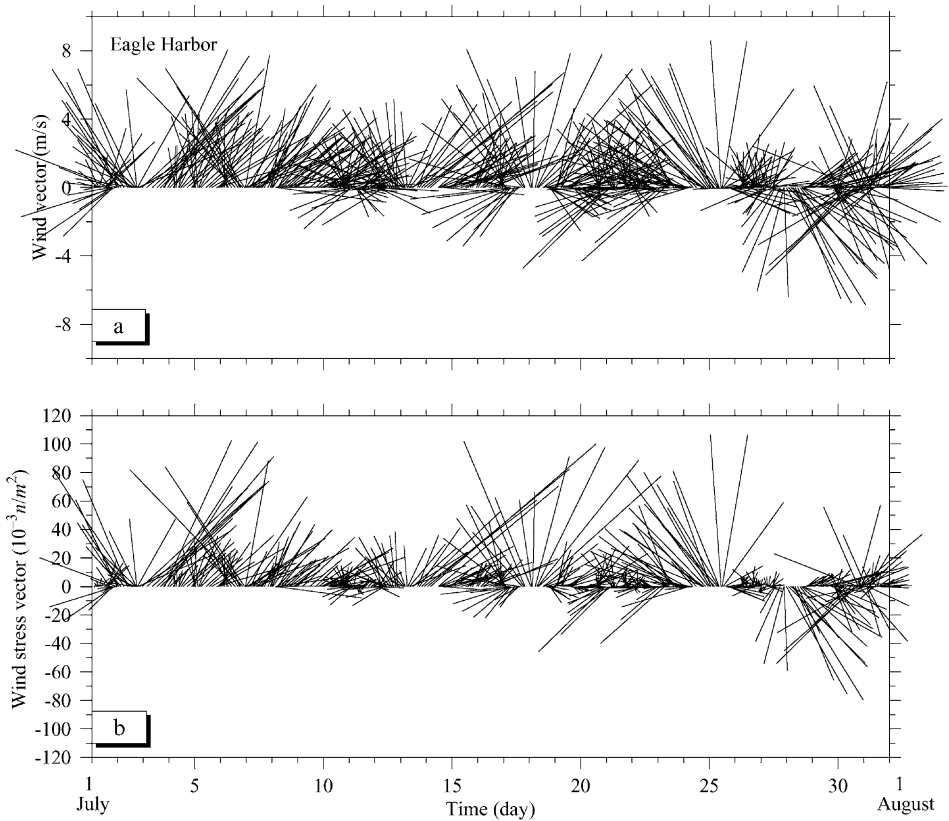


Fig. 4. Time series of observed wind (a), and calculated wind stress (b) vectors at Eagle Harbor for July 1973. The wind data were digitized from Fig. 3 in Niebauer et al. (1977).

coastal line, except on the eastern side of the Keweenaw Waterway outlet and near Eagle Harbor where the isobaths extended offshore (Fig. 5). The offshore movement of water particles was found throughout the whole water column at the northern end of transect A, east of the Keweenaw Waterway, even though they only accounted for a small portion of particles. Near Eagle Harbor, the cross-frontal offshore transport was evident near the offshore splitting area of the local isobaths, where offshore movement of water particles was found at depths below 20 m. A similar tendency of particle trajectories also was found for the case in which particles were released on transect B on the same day, suggesting that the cross-frontal water transport along the Keweenaw coast was topographically controlled (Fig. 6). To verify this finding, we released particles on transect C, a cross-shore section near the topographic-splitting area near Eagle Harbor on 3, 8, and 13 July during times the thermal front was intensified significantly by a northeastward wind. A large number of particles moved offshore on this section, no matter how the direction of the wind varied during the time after the particles released (Fig. 7).

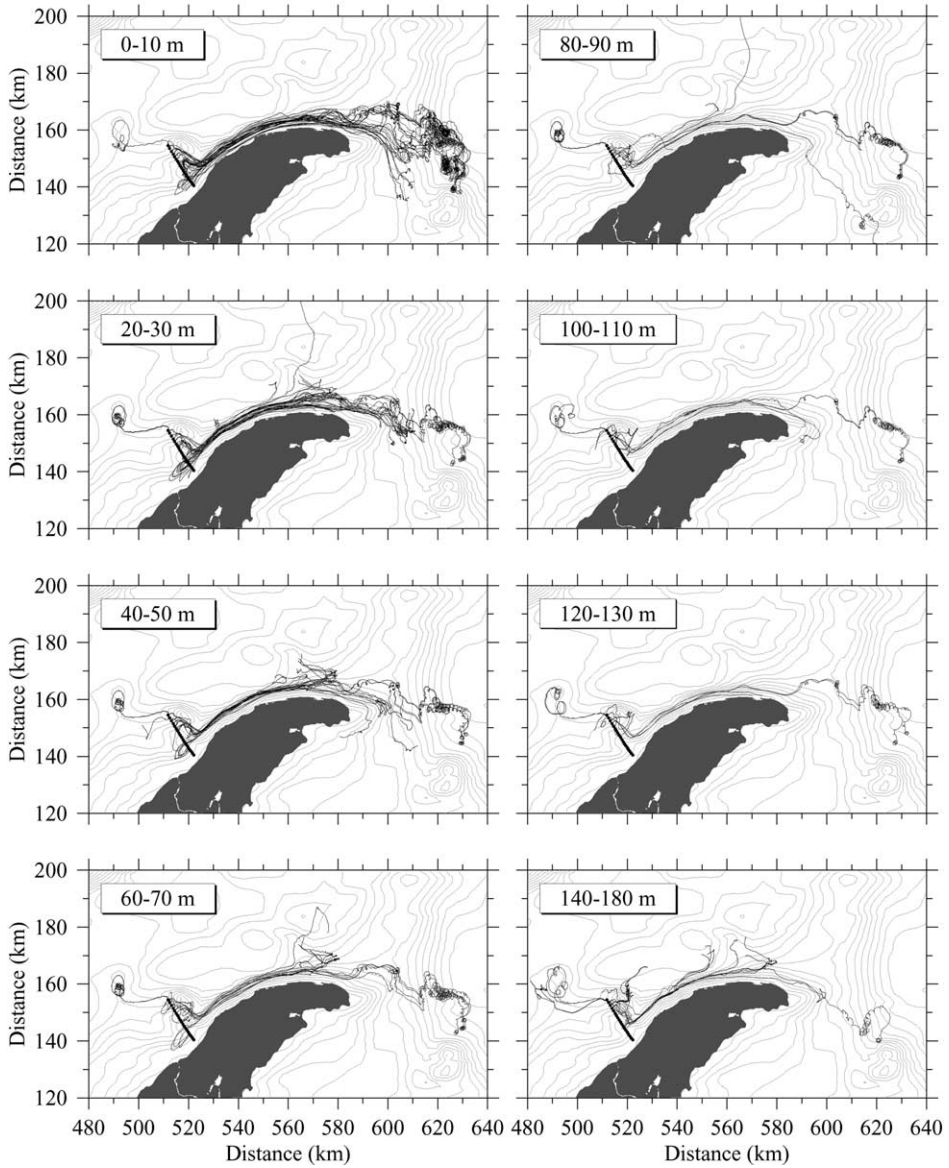


Fig. 5. Trajectories of particles that were released on transect A at the end of the second model day. The depth values shown in the upper left indicate the depth range in which the particles were released. Tracking time for all particles was 29 days starting on 2 July and ending on 31 July.

Tracking individual particles that were released from transects A and B, we found that the cross-frontal offshore movement of water particles near the topographic-splitting area near Eagle Harbor all occurred in the deep region no matter where they were released. For example, a particle, which was released at 20 m below the surface near the coast on

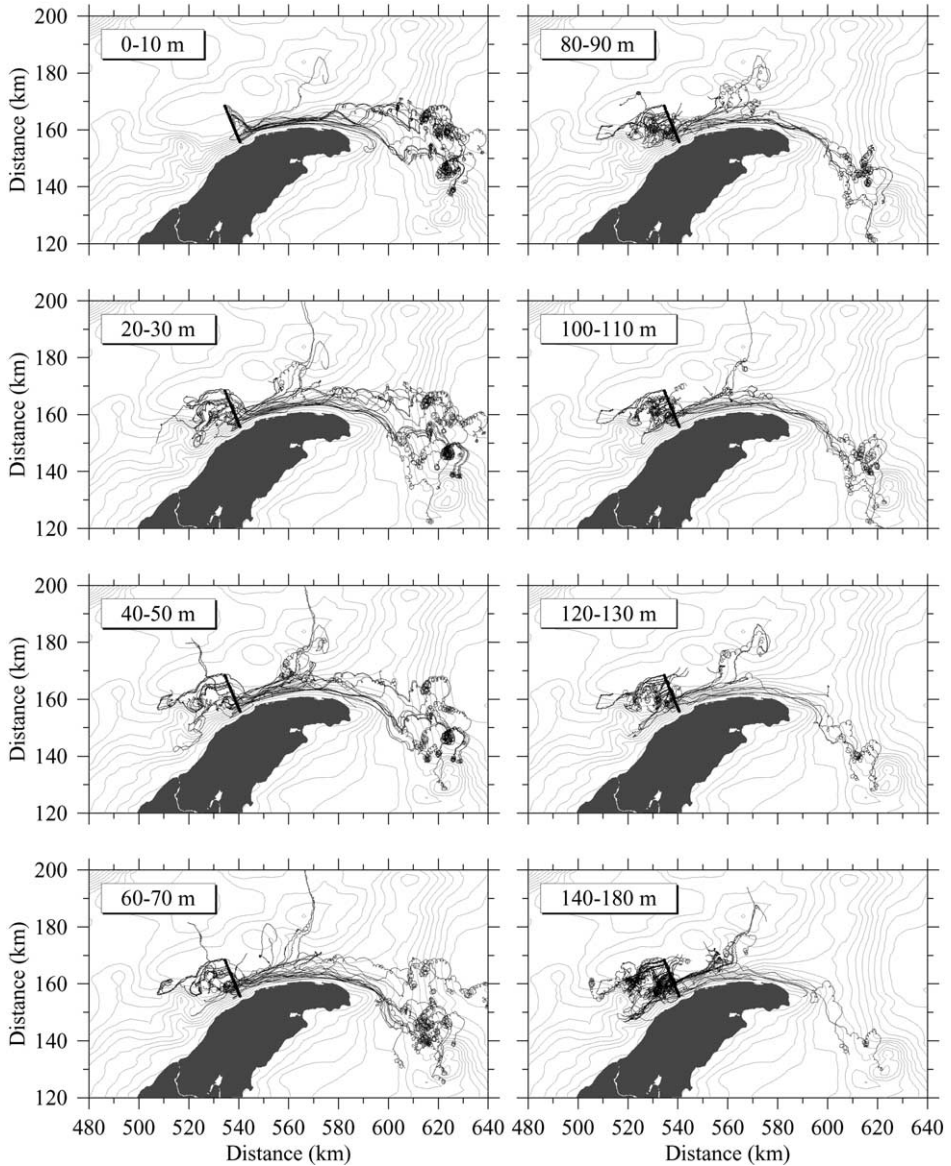


Fig. 6. Trajectories of particles that were released on transect B at the end of the second model day. The depth values shown in the upper left indicate the depth range in which the particles were released. Tracking time for all particles was 29 days starting on 2 July and ending on 31 July.

the second model day, shifted downward to 219 m when it moved eastward along the coast in the first 3 days, and moved offshore at about 200 m after 15 July (Fig. 8: upper panel). A similar trajectory also was found for a particle that was released at 90 m on transect A on the second model day. This particle first moved toward the coast in the

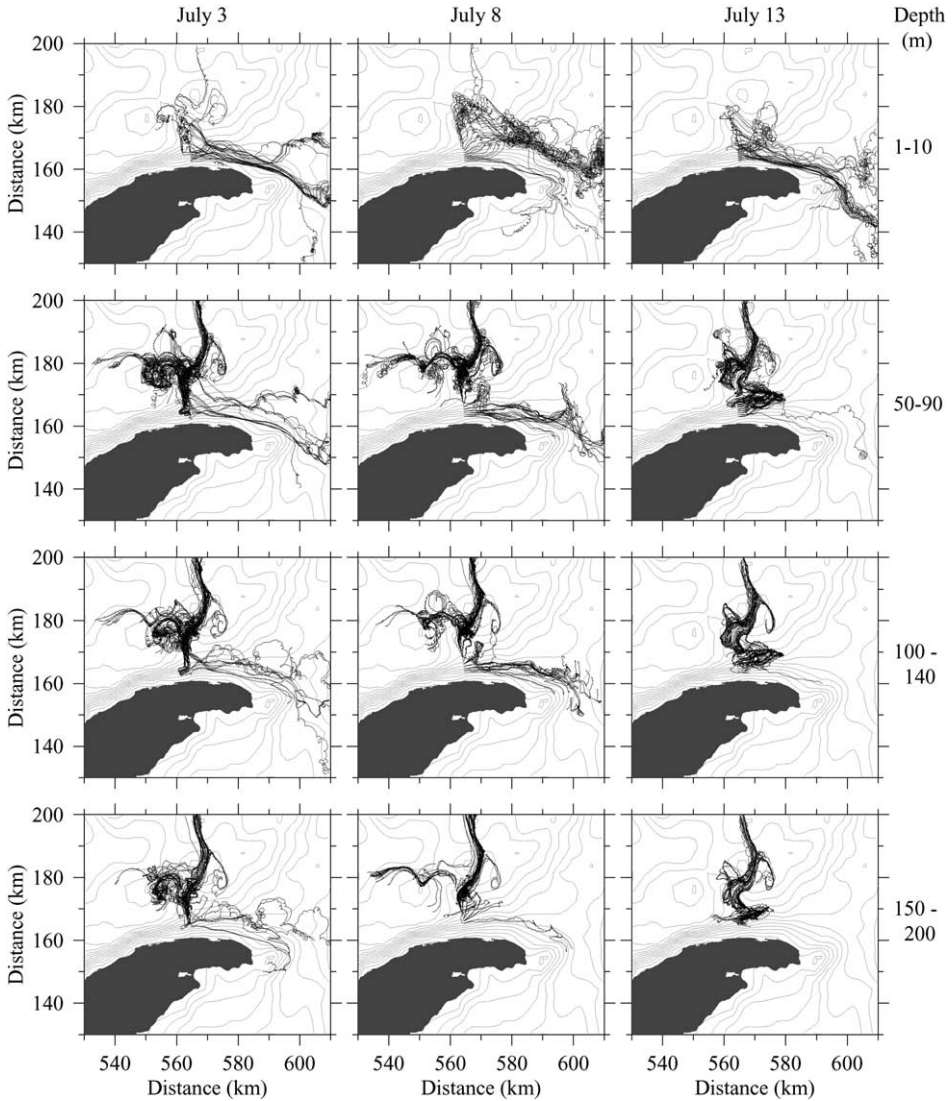


Fig. 7. Trajectories of particles that were released on transect C on 3 (left), 8 (middle), and 13 (right) July, respectively. The depth values shown in the lower right indicate the depth range in which the particles were released. The particles were tracked until the end of 31 July.

first 4 days, then moved along the coast for 6 days, and finally turned offshore at 183 m in the deep region after 15 July. Although there was the same evidence of cross-frontal offshore trajectories for particles in the upper 10 m when the particles were released on transect C, very close to the offshore topographic-splitting area, the majority of particles left offshore below 50 m. All these findings imply that a downward flow was dominant

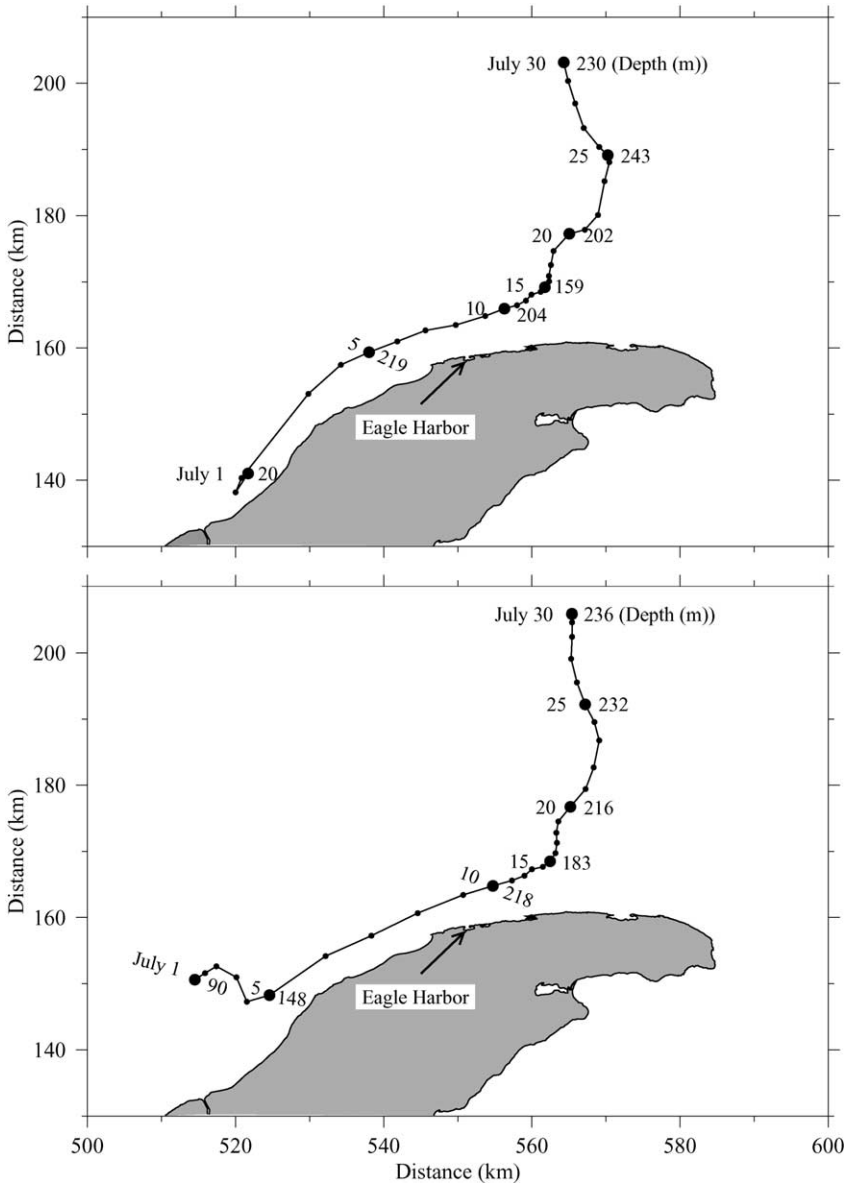


Fig. 8. Examples of the trajectories of the individual particles that were released at depth of 2 and 90 m below the surface on transect A on the second model day. The value on the left side of the trajectory is the tracking days and the value on the right side is the water depth (m) of the particle at that time. The water depth was calculated relative to the surface.

near the northern coast of the Keweenaw Peninsula in July 1973. A northeastward wind prevailed over the lake during July 1973. This wind tended to produce onshore water transports near the surface and hence caused downwelling against the coast. An offshore current was expected in the deep region based on the conservation of water mass. In addition to the topographically related driving mechanism (to be discussed later), this offshore deep current should also contribute directly to the offshore movement of particles in the deep region.

To examine the impacts of baroclinic instability of the thermal fronts and winds on the cross-frontal offshore transport associated with the Keweenaw Current, we tracked particles under idealized environments without and with the wind (note: in the no-wind case, heating was still retained). Removing the wind forcing from the current simulation the velocities of water particles were significantly reduced as a result of decreasing strength of the thermal frontal current (Chen et al., 2001). Most of particles which were released on transects A, B, and C tended to move along the coast, but a remarkable number of particles moved offshore at all depths around the offshore topographic-splitting area near Eagle Harbor (Fig. 9). This again supported our findings that the tendency for offshore movement of particles around the topographic-splitting area was mainly controlled by local bottom topography. Our previous studies have shown that the thermal front was baroclinically unstable when wind was removed from the system (Chen et al., 2001). Offshore meanders of temperature fields could occur in the area where the offshore splitting of bottom topography exists, leading to an offshore current there. The offshore movement of particles in this case was mainly due to the baroclinic instability of the thermal front over varying bottom topography in the along-shore direction. Since the offshore movement tendency of particles were observed over a time scale of 30 days, which was longer than the time scale of the offshore meander of temperature field (about 5 days), and also the tongue-like head part of offshore extended temperature contours tended to be separated from the thermal front a few days after meandering occurred, we believed that particles eventually left from the thermal front and entered into the interior of Lake Superior.

The wind did have a significant impact on the trajectories of water particles. Four experiments were conducted for the idealized wind cases in which a constant wind of 5 m/s blew from the southwest, northeast, northwest, and southeast directions, respectively (Fig. 10). In the case with a northeastward wind, at the surface, onshore Ekman transport pushed the particles to the coast. All the particles moved northeastward along the coast in the intensified Keweenaw Current and no surface particles left the shoreline (Fig. 10a: left). In the deep region below 50 m, however, several particles did leave the shore from the coast at the topographic-splitting area near Eagle Harbor (Fig. 10a: middle and right). In this case, the wind-induced mixed layer was less than 5 m and the wind tended to cause the offshore flow in the deep region as a result of mass conservation. However, since particles tended to leave offshore only over coastal bathymetry abutments, the wind seemed not to be the only physical process to cause such an offshore removal of water.

In the case with a southwestward wind, the wind resulted in an offshore Ekman transport in the upper mixed layer and hence a significant upwelling near the coast. As a result, at the surface, a large number of particles turned offshore in the direction of the wind-induced offshore Ekman transport (Fig. 10b: left). There were still significant offshore removals of particles along the northern coast of the Keweenaw Peninsula at 50 m below the surface (Fig. 10b:

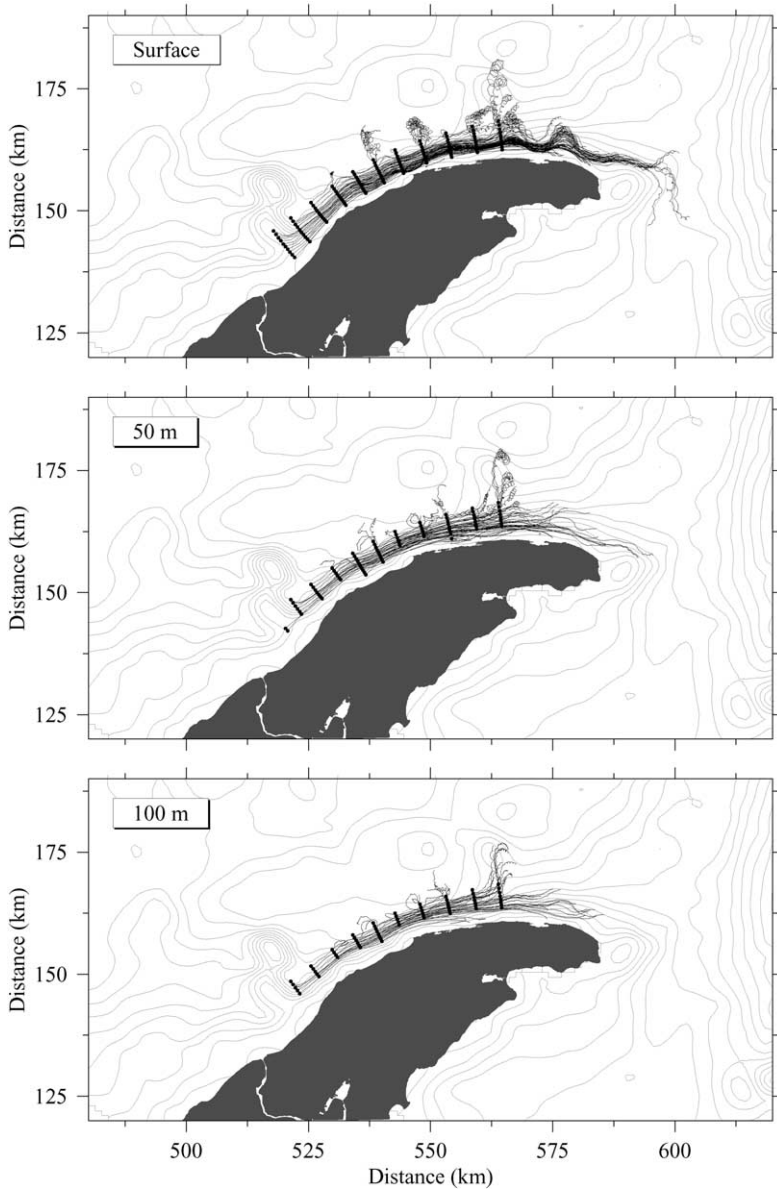


Fig. 9. Trajectories of particles that were released on several offshore transects within the Keweenaw Current on the second model day for the case without wind forcing. The heavy solid lines indicate that locations of the transects where the particles were released. Tracking time for all particles was 29 days starting on 2 July and ending on 31 July.

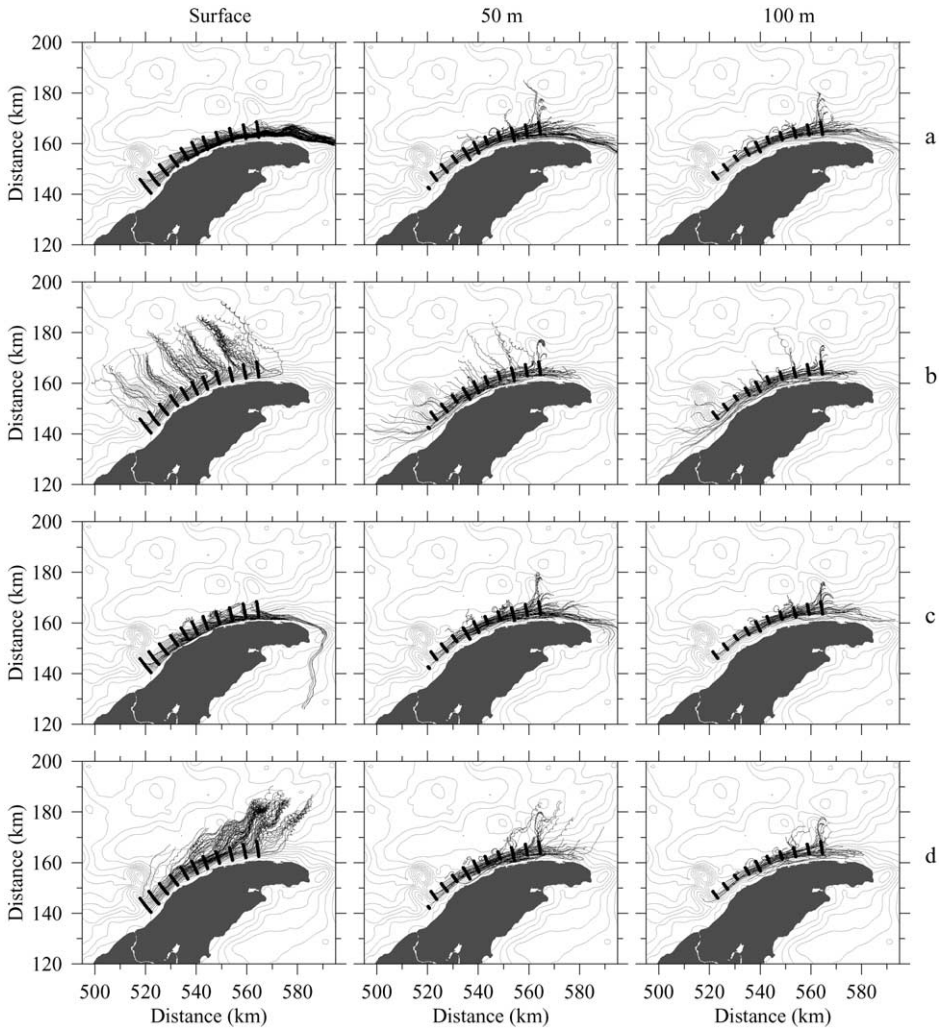


Fig. 10. Trajectories of particles that were released on several offshore transects within the Keweenaw Current on the second model day for the cases with northeastward (a), southwestward (b), southeastward (c), and northwestward (d) winds. The heavy solid lines in each figure and values on the top indicated that locations of transects and depths where the particles were released. Tracking time for all the particles was 29 days starting on 2 July and ending on 31 July.

middle). Offshore movement of particles also was evident at the topographic-splitting area near Eagle Harbor at 100-m depth (Fig. 10b: right).

In the case with a southeastward wind, at the surface, the wind-induced Ekman transport was southwestward onto the coast, which pushed particle against the coast and then moved them along the shore and thus no surface particles were found to leave the shore (Fig. 10c: left). In the deep region, the trajectories of particles were very similar to the case with a

northeastward wind, again showing clear evidence of offshore removals of particles at the topographic-splitting area near Eagle Harbor (Fig. 10c: middle and right).

In the case with a northwestward wind, the wind produced a northeastward Ekman transport in the upper mixed layer, which pushed all the surface particles to leave from the coast (Fig. 10d: left). The wind's effects were still evident at 50 m below the surface, where a significant number of particles moved offshore in the direction of the offshore Ekman transport (Fig. 10d: middle). In the deep region below 100 m, the offshore detachment of particles mainly occurred around the topographic-splitting point near Eagle Harbor, which was very similar to those found in the cases with the northeastward and southeastward winds (Fig. 10d: right).

Compared to the case without wind forcing, it is clear that the trajectories of particles near the surface followed the direction of wind-induced Ekman transport, but in the deep region they were mainly controlled by varying bottom topography. This explains why the particles in the deep region all tended to leave from the coast at the topographic-splitting area near Eagle Harbor, no matter where they were released or how the wind varied in July 1973.

4. The mechanism study

Particle trajectory tracking in the 3D flow field of July 1973 in Lake Superior has clearly shown that the particles, which were released in the distinct upstream of the Keweenaw Current, tended to leave the shore across the thermal front at the topographic-splitting area east of the Keweenaw Waterway and near Eagle Harbor. In particular, the particles frequently left the shorelines near Eagle Harbor in the deep region no matter at which depth they were released in the upstream or how the wind varied during that period. Numerical experiments for idealized wind fields have suggested that the tendency for offshore movement of particles in the deep region was closely related to varying bottom topography near Eagle Harbor. How was the offshore water transport related to the thermal front along the northern coast of the Keweenaw Peninsula? How did the structure of the thermal front vary with time under the real wind environment across varying bottom topography? These questions were addressed by examining the temporal and spatial variations of combined thermal structures and 3D field for the cases with real-time and idealized wind forcings.

In the real-time simulation for July 1973, offshore movement of particles usually concurred with an offshore meandering of the thermal front around the topographic-splitting area near Eagle Harbor. For example, a significant offshore meandering of the temperature field occurred throughout the water column below 50 m around the topographic-splitting area during the transition from southwestward to northeastward wind on 11 July (Fig. 11). At the surface, the northeastward wind tended to push the water against the coast on 14 July, and then caused an offshore transport on 17 July after the wind turned to the southeastward direction. In the deep region, the current turned to the offshore direction on 14 July as an offshore meandering of the thermal front developed. This offshore current drove the particles away from the coast and into the central basin of the lake.

The existence of offshore meandering of the thermal front in the mid- and deep regions probably is a result of vortex shedding off coastal bathymetry abutments which

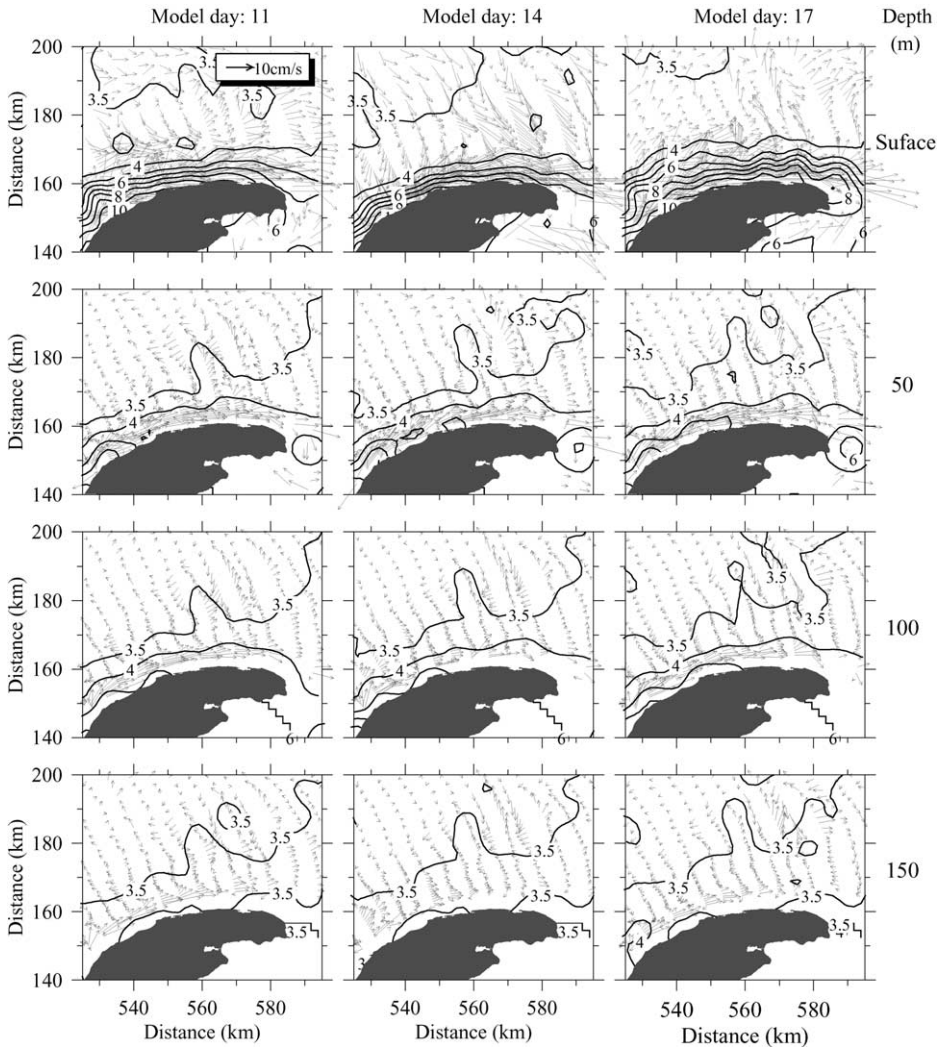


Fig. 11. Distributions of the model-simulated temperature and horizontal current vectors at the surface, 50, 100, and 150 m on the 11 (left), 14 (middle), and 17 (right) July.

is independent of the wind forcing. In the case without the wind, the offshore meandering of the temperature field occurred around the topographic-splitting area near Eagle Harbor in the deep region a few days after the establishment of the current jet through the Rossby adjustment process in which the density field adjusted to the flow field (Fig. 12). This was still true in the cases with constant northeastward, southwestward, southeastward and northwestward winds, suggesting that offshore meandering of the temperature field at the topographic-splitting area along the Keweenaw coast was a general feature of the thermal front over sloping bottom topography (Fig. 13).

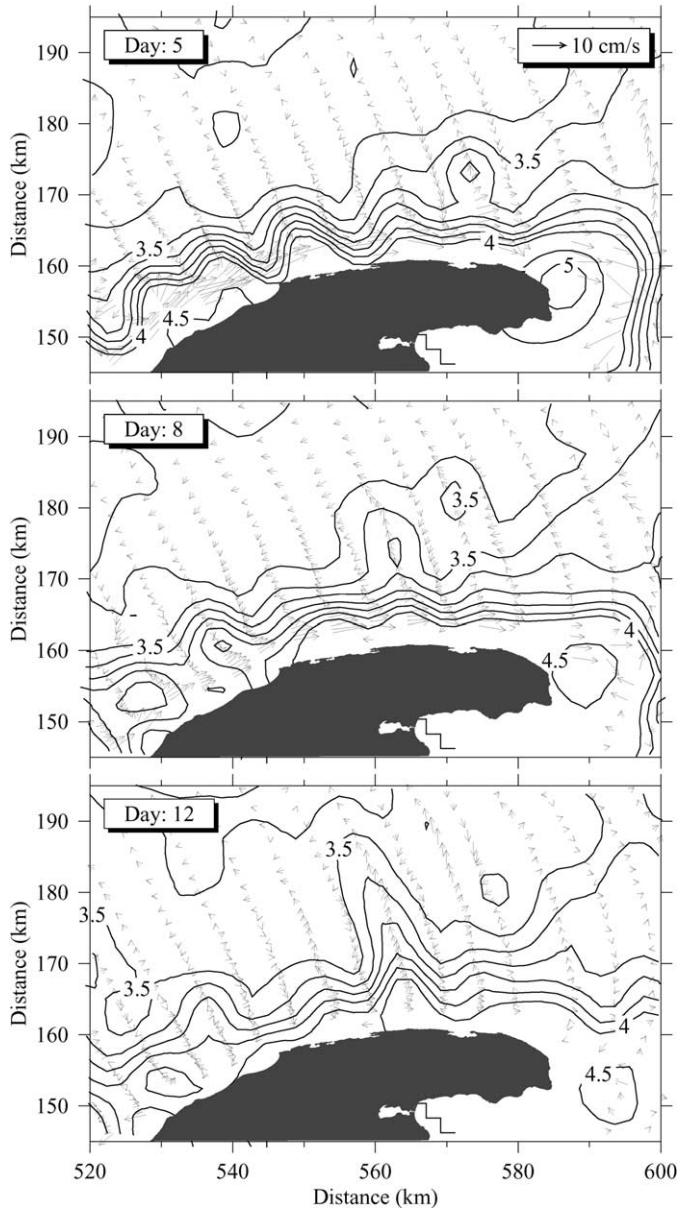


Fig. 12. Distributions of the model-simulated temperature and horizontal current vectors at 50 m below the surface on the fifth (upper), eighth (middle), and tenth (lower) model days for the case without wind forcing.

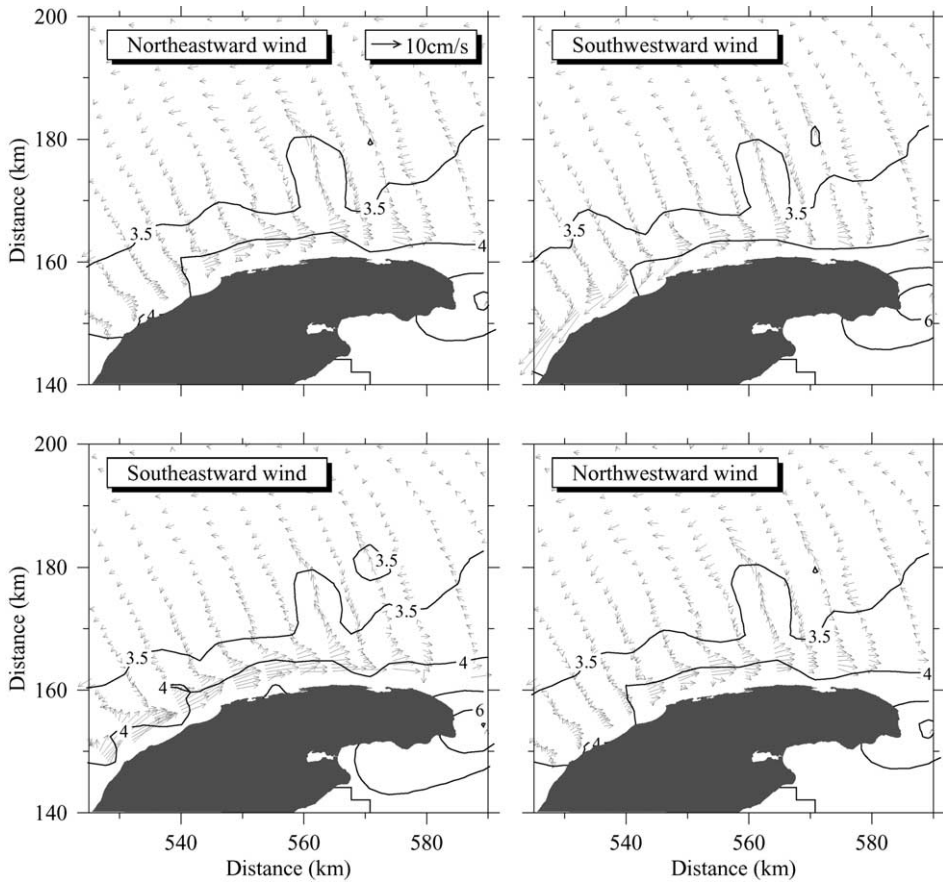


Fig. 13. Distributions of the model-simulated temperature and horizontal current vectors at 50 m below the surface on the eighth model days for the cases with northeastward (a), southeastward (b), southwestward (c), and northwestward (d) winds.

Diagnostic analysis of the momentum balance for the flow simulation of July 1973 in Lake Superior (Zhu et al., 2001) has revealed that both the along- and cross-shore currents in the deep region were approximately geostrophic. Offshore motion was mainly driven by along-shore surface elevation and baroclinic pressure gradients. Under the geostrophic condition, the potential vorticity remained conservative along the trajectory of a particle. Without considering thermal effects, a particle in the Keweenaw Current should follow the local isobath along the northern coast of the Keweenaw Peninsula since the Coriolis parameter (planetary vorticity) f remained almost constant in such a small region. When the offshore meandering of temperature field occurred, a vortex shedding off the coastal bathymetry abutment near Eagle Harbor produced a cyclonic vorticity in the flow field, which tended to make particles move offshore to the deep region in order to maintain conservative potential vorticity.

Chen et al. (2001) examined the stability of the thermal front associated with the Keweenaw Current. They found that this front was baroclinically unstable under windless conditions. In these cases, the thermal front tended to diffuse gradually and no equilibrium state of thermal structure could be reached. For the idealized windless case in our current study, heating was included to maintain the development of thermal front along the coast. In such a case with external forcing, the baroclinic instability was probably a key process that caused an offshore meander of the temperature field around the topographic-splitting area near Eagle Harbor. This mechanism was still applied for the cases with idealized wind forcing since the offshore meandering of temperature fields in the deep region was not altered after the wind was added.

5. Conclusion

Offshore water transport across the thermal front along the Keweenaw coast in Lake Superior was examined by tracking the trajectories of water particles in model-simulated 3D flow field of July 1973. Particles were released every 10 m in the vertical on cross-shore transects A, B, and C on the 2, 7, 12, and 22 July and tracked until the end of the month. The trajectories of particles revealed a remarkable offshore water transport at the topographic-splitting area on the east of the Keweenaw Waterway and near Eagle Harbor. The model results showed that the northern coast of the Keweenaw Peninsula in July of 1973 was dominated by wind-induced downwelling. The particles, which were released upstream in the Keweenaw Current, tended to move downward when they were advected along the coast by the current jet and were likely to turn offshore in the deep region near Eagle Harbor. Offshore movement of particles in the deep region also was evident in windless conditions and cases with constant northeastward, southwestward, southeastward, and northwestward winds, respectively.

The model-predicted offshore movement tendency of particles is in good agreement with the distribution of suspended sediment along the Keweenaw coast (personal communication with Noel Urban and Erik Brown). Offshore cross-frontal transport along the northern coast of the Keweenaw Peninsula was driven dominantly by wind-induced Ekman flow near the surface but was controlled by the local bottom topography in the deep region. A northeastward wind prevailed over the lake during July 1973. This wind tended to produce onshore water transports near the surface and hence caused downwelling against the coast. An offshore current was expected in the deep region based on the conservation of water mass. Vortex shedding off coastal bathymetry abutments plus baroclinic instability of the thermal front led to offshore meandering of the temperature field in the deep region over local varying bottom topography. This meandering tended to produce a cyclonic vorticity and drove particles offshore across the thermal front.

Acknowledgements

This research was supported by the National Science Foundation under grant number OCE-9712869; OCE-0196543 for Changsheng Chen, OCE-9712871 for Elise Ralph, and

OCE-9712872 for Sarah Green and Judy Budd. We would like to thank four anonymous reviewers for their many constructive suggestions.

References

- Bennett, E.B., 1978. Characteristics of the thermal regime of Lake Superior. *J. Great Lakes Res.* 4 (3/4), 310–319.
- Blanton, J.O., Oey, L.Y., Amft, J., Lee, T.N., 1989. Advection of momentum and buoyancy in a coastal frontal zone. *J. Phys. Oceanogr.* 19, 98–115.
- Blumberg, A.F., Mellor, G.L., 1987. A description of a three-dimensional coastal ocean circulation model. *Three-Dimensional Coastal Models Am. Geophys. Union, Coastal and Estuarine Sciences, Vol. 4*, 1–16.
- Chao, S.Y., 1987. Wind-induced motion near the inner shelf fronts. *J. Phys. Oceanogr.* 16, 2137–2149.
- Chen, C., Zheng, L., Blanton, J., 1999. Physical processes controlling the formation, evolution, and perturbation of the low-salinity front in the inner shelf off the southeastern US: a modeling study. *J. Geophys. Res.* 104, 1259–1288.
- Chen, C., Zhu, J., Ralph, E., Green, S.A., Budd, J.W., Zhang, F.Y., 2001. Prognostic modeling studies of the Keweenaw Current in Lake Superior. Part I. Formation and evolution. *J. Phys. Oceanogr.* 31, 379–395.
- Mellor, G.L., Yamada, T., 1982. Development of a turbulence-closure model for geophysical fluid problem. *Rev. Geophys. Space Phys.* 20, 851–875.
- Niebauer, H.J., Green, T., Ragotzkie, R.A., 1977. Coastal upwelling/downwelling cycles in southern Lake Superior. *J. Phys. Oceanogr.* 7 (6), 918–927.
- Oey, L.Y., 1986. The formation and maintenance of density fronts on the US southeastern continental shelf during winter. *J. Phys. Oceanogr.* 16, 1121–1135.
- Qiu, B., Imasato, N., 1988. Baroclinic instability of buoyancy-driven coastal density currents. *J. Geophys. Res.* 93, 5037–5050.
- Smith, N.P., Ragotzkie, R.A., 1970. A comparison of computed and measured currents in Lake Superior. In: *Proceedings of the 13th Conference on Great Lakes Research*, pp. 969–977.
- Zhu, J., Chen, C., Ralph, E., Green, S.A., Budd, J.W., Zhang, F.Y., 2001. Prognostic modeling studies of the Keweenaw Current in Lake Superior. Part II. Simulation. *J. Phys. Oceanogr.* 31, 396–410.